



clonic seizures in humans (Denac *et al.* 2000; Stafstrom 2007) and in *in vitro* and *in vivo* models of ischemia (Taylor and Meldrum 1995).

It has been well-established that homeostasis of  $\text{Na}^+$  and  $\text{Ca}^{2+}$  is tightly coupled in neurons (Kiedrowski *et al.* 1994; Kiedrowski and Costa 1995; White and Reynolds 1995). Massive  $\text{Na}^+$  influx leads to a deleterious increase of intracellular  $\text{Ca}^{2+}$  concentration ( $[\text{Ca}^{2+}]_i$ ), which activates proteases, lipases and endonucleases and causes reactive oxygen species overproduction that underlies neuronal damage in epilepsy and ischemic stroke (Tymianski and Tator 1996; DeLorenzo *et al.* 2006; Fekete *et al.* 2008). The specific interaction between an increased level of  $I_{\text{Na,P}}$  and neuronal  $\text{Ca}^{2+}$  homeostasis, however, has yet to be elucidated in hippocampal CA1 pyramidal neurons. Moreover, the mechanism of the  $[\text{Ca}^{2+}]_i$  increase and its temporal pattern have not been well explored either. Understanding of the complex interaction of  $I_{\text{Na,P}}$  and neuronal  $\text{Ca}^{2+}$  sources requires the measurement of membrane potential ( $E_m$ ), intracellular  $\text{Na}^+$  concentration ( $[\text{Na}^+]_i$ ) and  $[\text{Ca}^{2+}]_i$  (i.e., the important parameters of neuronal excitability) under the same experimental conditions.

To investigate the action of increased  $I_{\text{Na,P}}$  on  $[\text{Ca}^{2+}]_i$ , we applied the  $I_{\text{Na,P}}$  activator veratridine to acute hippocampal slices (Ulbricht 1965, 2005; Alkadhi and Tian 1996). Veratridine, by binding to the neurotoxin receptor site 2 of VGSCs, inhibits VGSC inactivation and shifts the channel activation threshold toward a more negative membrane potential (Denac *et al.* 2000; Ulbricht 2005). Binding site 2 is also the target of some antiepileptic drugs such as carbamazepine and phenytoin (Willow and Catterall 1982; Worley and Baraban 1987), which also show neuroprotective action (Taylor and Meldrum 1995). Veratridine induces  $\text{Na}^+$  influx (Deri and Adam-Vizi 1993; Rose and Ransom 1997) and toxicity in both neuronal cultures (Pauwels *et al.* 1989) and hippocampal slices (Malgouris *et al.* 1994).

Using rat hippocampal slices, we show that the underlying mechanisms for increased  $I_{\text{Na,P}}$ -evoked elevation of  $[\text{Ca}^{2+}]_i$  in CA1 pyramidal cell somata are the influx of  $\text{Ca}^{2+}$  through the voltage-gated  $\text{Ca}^{2+}$  channels (VGCCs), reverse operation of the  $\text{Na}^+-\text{Ca}^{2+}$  exchanger (NCX) and the net effect of mitochondrial  $\text{Ca}^{2+}$  uptake and release. These components contribute to the  $\text{Ca}^{2+}$  signal with different temporal patterns. We also show that the endoplasmic reticulum (ER) does not amplify this response. Since the veratridine-evoked depolarization and AP bursting of CA1 pyramidal cells in slices is an *in vitro* model of epilepsy (Tian *et al.* 1995; Otoom *et al.* 1998) and  $\text{Ca}^{2+}$  increase presumably plays an important role in the genesis and maintenance of epileptiform activity (DeLorenzo *et al.* 2006), the understanding of the precise mechanism of  $I_{\text{Na,P}}$ -evoked  $\text{Ca}^{2+}$  increase may also contribute to the development of novel treatments for epilepsy.

## Materials and methods

### Acute hippocampal slice preparation

Procedures were performed in accordance with the National Institutes of Health guidelines for the care and use of animals and were approved by the Institutional Animal Care and Use Committee. Male Wistar rats, 16–21 days old, were anesthetized using xylazine/ketamine and decapitated. The brain was removed and placed in ice-cold cutting solution (composition in mM: NaCl, 126; KCl, 2.5;  $\text{NaHCO}_3$ , 26;  $\text{CaCl}_2$ , 0.5;  $\text{MgCl}_2$ , 5;  $\text{NaH}_2\text{PO}_4$ , 1.25; and glucose, 10) that was continuously bubbled with 95%  $\text{O}_2$  + 5%  $\text{CO}_2$  to produce a pH of 7.4. Thick coronal slices (250  $\mu\text{m}$ ) were cut with a vibratome (Vibratome 1000, TPI, St. Louis, MO, USA), separated into left and right halves, and transferred into a mesh-bottom holding chamber containing artificial cerebrospinal fluid (in mM: NaCl, 126; KCl, 2.5;  $\text{NaHCO}_3$ , 26;  $\text{CaCl}_2$ , 2;  $\text{MgCl}_2$ , 2;  $\text{NaH}_2\text{PO}_4$ , 1.25; and glucose, 10) bubbled with a mixture of 95%  $\text{O}_2$  + 5%  $\text{CO}_2$  (pH 7.4). After 20–25 min incubation at 32.5°C, the slices were kept at 25°C for the rest of the experiment.

### $[\text{Ca}^{2+}]_i$ measurement

The slices were incubated in 5  $\mu\text{M}$  fura-2AM (Grynkiewicz *et al.* 1985) at 25°C for 50 min. The loading solution contained 0.025% (w/v) of the neutral detergent Pluronic F-127. Slices were superfused with artificial cerebrospinal fluid (2 mL/min;  $\text{NaH}_2\text{PO}_4$  was omitted in experiments with  $\text{CdCl}_2$ ) in an experimental chamber mounted on a Gibraltar BX1 platform (Burleigh) and viewed with a 40 $\times$  water immersion objective on an Olympus BX50WI upright microscope. Pyramidal cells of the CA1 region were illuminated (340  $\pm$  5 nm and 380  $\pm$  5 nm) with a Polychrome II monochromator (TILL Photonics). The emitted light (510  $\pm$  20 nm) was detected by a cooled CCD camera (Photometrics Quantix, Tucson, AZ, USA), and the system was controlled by the Axon Imaging Workbench 4.0 software (Axon Instruments, Union City, CA, USA). Cell image intensities were background-corrected using a nearby area devoid of loaded cells. Values of  $[\text{Ca}^{2+}]_i$  in the cell somata were calculated off-line (Grynkiewicz *et al.* 1985):  $[\text{Ca}^{2+}]_i = K_d \times F_{\text{max}380}/F_{\text{min}380} \times (R - R_{\text{min}})/(R_{\text{max}} - R)$ , where  $R$  is the actual ratio of emission intensity at 340 nm excitation to emission intensity at 380 nm excitation,  $R_{\text{min}}$  and  $R_{\text{max}}$  are the same ratios at 0 mM or saturating  $[\text{Ca}^{2+}]$ , respectively and  $F_{\text{max}380}$  and  $F_{\text{min}380}$  are the fluorescence intensities for 0 mM or saturating  $[\text{Ca}^{2+}]$  at 380 nm excitation, respectively. The parameters  $K_d$ ,  $F_{\text{max}380}/F_{\text{min}380}$ ,  $R_{\text{min}}$ , and  $R_{\text{max}}$  were determined by the Calcium Calibration Buffer Kit with Magnesium #2.

### $[\text{Na}^+]_i$ measurement

Slices were loaded with 10  $\mu\text{M}$  SBFI/AM (Minta and Tsien 1989) at 25°C for 60 min and then deesterified for 90 min. We added 0.05% (w/v) Pluronic F-127 (Molecular Probes, Eugene, OR, USA) to promote dye loading. Minta and Tsien (1989) described SBFI as a dual wavelength dye, however, bulk loading of CA1 pyramidal cells in our brain slice preparations resulted in a single wavelength characteristic (see absorption spectra at 0 and 130 mM  $[\text{Na}^+]$  in Fig. 2b). The spectral properties of SBFI are highly dependent on the environment (e.g., viscosity, ionic strength, temperature). Our finding is consistent with the results of other groups that have demonstrated that intensity decreases in the entire spectrum as  $[\text{Na}^+]$

increases (Negulescu and Machen 1990; Borzak *et al.* 1992). We therefore performed single wavelength excitation. We illuminated our slices at  $365 \pm 5$  nm (i.e., the highest ratio of Na<sup>+</sup>-free to Na<sup>+</sup>-bound fluorescence; Fig. 2b). The emitted light was detected ( $510 \pm 20$  nm) by a cooled CCD camera as described above. Image intensities over cell bodies were exponentially-corrected (because of dye bleaching) after background subtraction. The [Na<sup>+</sup>]<sub>i</sub> concentrations of the cell somata was calculated off-line as follows (Grynkiewicz *et al.* 1985):  $[\text{Na}^+]_i = K_d \times (F - F_{\min}) / (F_{\max} - F)$ , where  $F$  is the actual emission intensity at 365 nm excitation,  $F_{\min}$  is the fluorescence intensity at the lowest [Na<sup>+</sup>]<sub>i</sub> at 365 nm excitation and  $F_{\max}$  is the fluorescence intensity at saturating [Na<sup>+</sup>]<sub>i</sub> at 365 nm excitation.  $F_{\max}$  and  $F_{\min}$  values were determined *in situ* at the end of every individual experiment (Fig. 2c inset). We measured  $F_{\min}$  after at least 15 min application of calibration media containing 0 mM Na<sup>+</sup>, 155 mM K<sup>+</sup> and 10 μM gramicidin D (monovalent cation ionophore; Fig. 2c inset).  $F_{\max}$  was measured at the beginning of the perfusion of the same calibration media, as it depolarizes the cells and induces a massive Na<sup>+</sup> influx attributable to its high potassium content and the still high extracellular [Na<sup>+</sup>] that needs time to be washed out (Fig. 2c inset).  $K_d$  was calculated from nine-point *in situ* calibrations ([Na<sup>+</sup>] in mM: 0, 3, 6, 10, 20, 40, 80, 130, 155) made in CA1 pyramidal cells of the acute hippocampal slices ( $K_d = 17.855$  mM;  $n = 10$ ). The calibration media contained (in mM) 0.6 MgCl<sub>2</sub>, 0.5 CaCl<sub>2</sub>, 10 HEPES, 10 glucose and 0.01 gramicidin D. The [Na<sup>+</sup> + K<sup>+</sup>] was equal to 155 mM, Cl<sup>-</sup> was 30 mM and gluconate was 125 mM (Harootunian *et al.* 1989; Diarra *et al.* 2001). Electrical field stimulations were delivered through two platinum wires (10 Hz, 50 shocks, 45 V/cm).

### Electrophysiology

Pyramidal neurons of the CA1 hippocampal subfield were visualized by differential interference contrast microscopy (DIC). Patch pipettes were pulled from borosilicate glass (1.2 mm OD; Harvard Instruments, March-Hugstetten, Germany). For current-clamp recordings, 5–9 MΩ electrodes were filled with (in mM) 125 K-gluconate, 20 KCl, 10 HEPES, 10 Di-Tris-salt phosphocreatine, 0.3 Na-GTP, 4 Mg-ATP, 10 NaCl. Cells with an initial resting membrane potential that was more negative than -50 mV were accepted. Data acquisition and analysis were performed using pClamp8 (Axon Instruments, Foster City, CA, USA).

### Data analysis

The effect of the drugs on the veratridine-evoked [Ca<sup>2+</sup>]<sub>i</sub> increase was evaluated by comparing the peak responses in the presence and absence of the drugs. In experiments in which the drug treatment abolished the peak(s), the values corresponding to the peaks were taken at the average peak<sub>1</sub> (10 s) and peak<sub>2</sub> (80 s) times determined in the control experiments. Only neurons with stable [Ca<sup>2+</sup>]<sub>i</sub> baselines and healthy morphologies in DIC images were included in the statistical analysis. The “*n*” values show the number of cells, slices and animals (e.g., *n* of cells/slices/animals). Since the delay of response after the start of veratridine perfusion may vary from cell to cell (consider diffusion in slice and that veratridine inhibits the inactivation of VGSCs; see, e.g., Otoom *et al.* 1998) the starting point of the response is indicated by an arrow. When there are more traces on a figure, they are set according to the starting point. Data are presented as mean ± SEM.

Statistical analysis was performed using one-way ANOVA with Dunnett's *post-hoc* test unless otherwise noted. Differences were considered significant at *p*-values < 0.05.

### Materials

The following chemicals were used: sodium-binding benzofuran isophthalate (SBFI/AM), fura-2AM, Pluronic F-127 and Calcium Calibration Buffer Kit with Magnesium #2 (Molecular Probes); veratridine, DL-2-amino-5-phosphonopentanoic acid (AP-5), 6-cyano-7-nitroquinoxaline-2,3-dione disodium salt (CNQX), CdCl<sub>2</sub>, gramicidin D, HEPES, nifedipine, NiCl<sub>2</sub>, carbonyl cyanide 3-chlorophenylhydrazone (CCCP) and EGTA (Sigma Chemical Co., St. Louis, MO, USA); ω-conotoxin-MVIIIC, CGP-37157, 2-[2-[4-(4-nitrobenzyloxy) phenyl]]isothiourea (KB-R7943), cyclosporine A (CsA; Tocris, Ballwin, MO, USA); thapsigargin (Alomone Labs, Jerusalem, Israel). All other chemicals were purchased from Merck (Darmstadt, Germany).

## Results

### Veratridine evokes a biphasic [Ca<sup>2+</sup>]<sub>i</sub> elevation in CA1 pyramidal neurons

We measured the [Ca<sup>2+</sup>]<sub>i</sub> of fura-2AM loaded CA1 pyramidal neurons in acute hippocampal slices. Administration of veratridine (10 μM, 1 min) to the perfusion buffer generated a biphasic Ca<sup>2+</sup> response in the somata (Fig. 1a). The first peak was smaller and steeply rising (peak<sub>1</sub> = 241.5 ± 24.9 nM, peak<sub>2</sub> = 616.2 ± 68.9 nM;  $n = 38/19/18$ ). The first and second peaks came 10.4 ± 1.0 and 80.3 ± 5.2 s later than the beginning of the veratridine response, respectively. Resting [Ca<sup>2+</sup>]<sub>i</sub> was 56.6 ± 3.7 nM ( $n = 201/78/57$ ). Ca<sup>2+</sup>-free media, containing 1 mM EGTA abolished both [Ca<sup>2+</sup>]<sub>i</sub> peaks, suggesting an extracellular source of [Ca<sup>2+</sup>]<sub>i</sub> elevation ( $n = 8/5/5$ ;  $p < 0.05$ , unpaired *t*-test; Fig. 1a). We previously showed that the selective and potent VGSC inhibitor TTX (1 μM) abolishes the veratridine-induced [Ca<sup>2+</sup>]<sub>i</sub> response (Zelles *et al.* 2001). Blockade of VGSCs by TTX interferes with both the direct (i.e., on the imaged cell) and indirect (through other connected neurons) action of veratridine. In order to determine the involvement of the indirect stimulatory effect in the overall response, we inhibited the excitatory glutamate inputs by using NMDA and AMPA/kainate receptor inhibitors AP-5 (50 μM) and CNQX (30 μM), respectively. Combined application of AP-5 and CNQX did not significantly influence the peaks, indicating the dominance of the direct action of veratridine on the neurons (peak<sub>1</sub> = 319.5 ± 56.6 nM;  $p > 0.05$ ; peak<sub>2</sub> = 894.6 ± 189.5 nM;  $p > 0.05$ ;  $n = 15/6/4$ ; see Figs 3a, 4a and b).

### Veratridine induces depolarization and firing of neurons

Somatic whole-cell current-clamp recordings showed the effect of veratridine perfusion (10 μM, 1 min) on electrical properties of CA1 pyramidal neurons ( $n = 7/7/5$ ; Fig. 1b and c). The veratridine response typically started with a massive

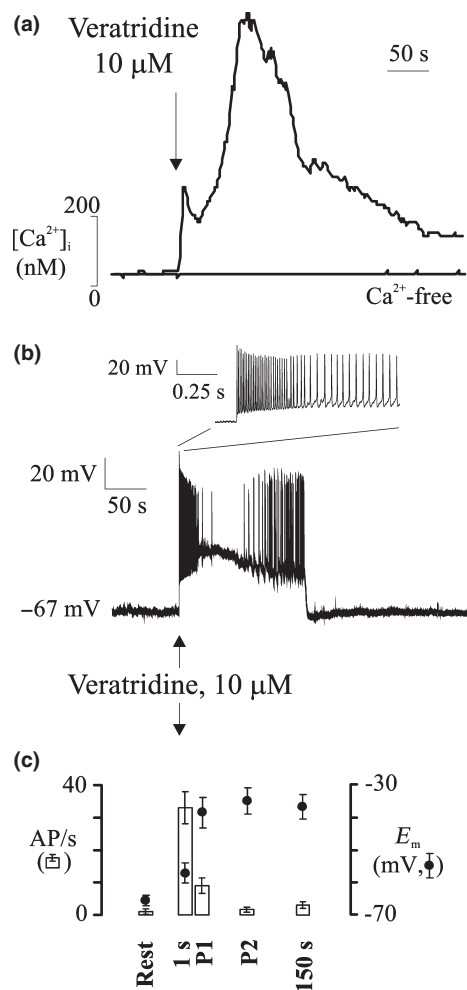


**Fig. 1** Inhibition of VGSC inactivation by veratridine (10  $\mu\text{M}$ , 1 min perfusion) elevates  $[\text{Ca}^{2+}]_i$  and evokes AP firing and depolarization of CA1 pyramidal neurons. (a) Representative traces show the biphasic  $\text{Ca}^{2+}$  response and its elimination in  $\text{Ca}^{2+}$ -free ACSF. (b) The representative trace demonstrates the massive firing in the initial phase of the response (see the enlargement of the 1st s in the inset) and the dependence of AP frequency on  $E_m$ . (c) The diagram shows the average level of membrane potential ( $E_m$ , dots with the right scale bar) and firing rates (AP/s, column bars with the left scale bar) at certain characteristic time points of the veratridine response (Rest: resting level; 1 s: 1st s of AP burst; P1: 10th s, characteristic time of the first  $[\text{Ca}^{2+}]_i$  peak; P2: 80th s, characteristic time of the second  $[\text{Ca}^{2+}]_i$  peak; 150 s: 150th s). The start of the veratridine effect is indicated by the arrows.  $[\text{Ca}^{2+}]_i$  and  $E_m$  were measured in different neurons, the traces and subfigure C were adjusted in time according to the start of the veratridine response. Timescales are identical.

firing of neurons (Fig. 1b inset). The firing rate depended on the  $E_m$ , which showed a plateau-like depolarization followed by an oscillation. Figure 1c illustrates the average levels of  $E_m$  and firing rates at certain characteristic time points of the response. The resting membrane potential (Rest) was  $-64.0 \pm 3.9$  mV. Veratridine application induced a

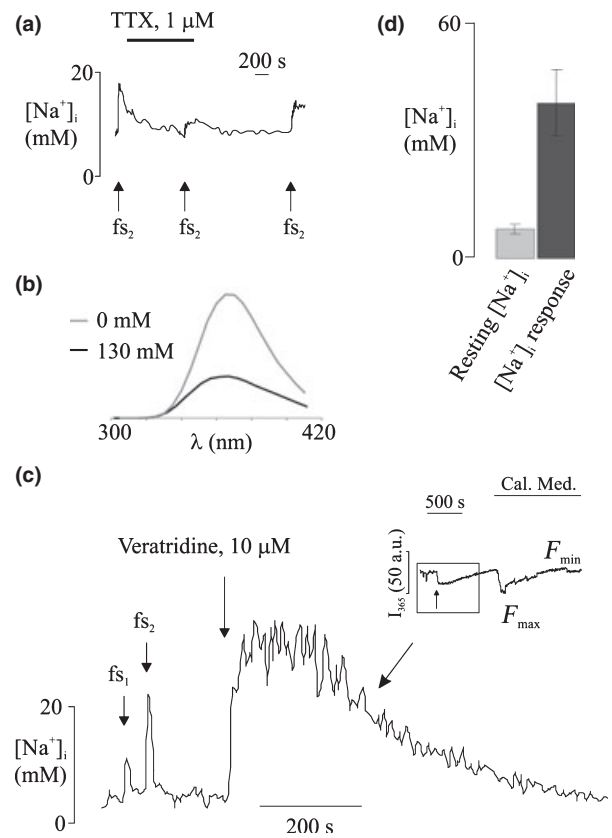
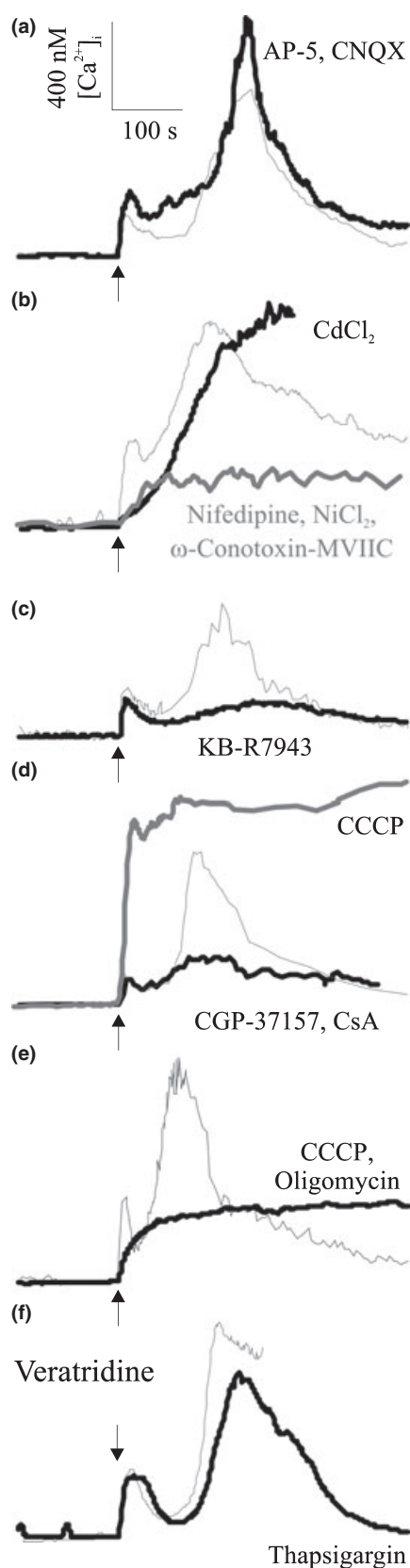


**Fig. 2** Measurement of veratridine effect on  $[\text{Na}^+]_i$  in CA1 pyramidal neurons in acute hippocampal slices. (a) The electric field stimulation-evoked elevation of  $[\text{Na}^+]_i$  is inhibited by TTX (1  $\mu\text{M}$ ). The response recovered after washout of the toxin (representative of  $n = 4/2/2$ ). (b) Increasing the extracellular  $[\text{Na}^+]$  from 0 mM (gray line) to 130 mM (black line) in the presence of gramicidin D (10  $\mu\text{M}$ ) induced a decrease in fluorescence in the excitation spectra measured every 5 nm ( $\lambda$ ; wavelength). Slices were loaded with SBF1/AM (representative trace of three identical experiments). (c) Veratridine (10  $\mu\text{M}$ , 1 min perfusion) induced a large, monophasic  $[\text{Na}^+]_i$  increase as shown by the representative trace. The start of the veratridine effect is indicated by the long arrow. Short arrows indicate electric field stimulations with 1 ( $fs_1$ ) and 2 ms ( $fs_2$ ) impulse duration, respectively. Calibration was performed *in situ* following every experiment with a calibration media (Cal. Med.; see Materials and methods). Raw intensity curve of the same experiment following background subtraction and exponential correction of dye bleaching is illustrated in the inset. (Arrow, start of the veratridine response; a.u., arbitrary units of emitted intensity at 365 nm excitation ( $I_{365}$ );  $F_{\min}$  and  $F_{\max}$ , fluorescent intensities at the lowest and at saturating  $[\text{Na}^+]_i$ , respectively). (d) The column bar indicates the level of resting (light gray column) and peak  $[\text{Na}^+]_i$  following veratridine administration (dark gray column).

spontaneous membrane depolarization to  $-56.6 \pm 2.8$  mV, which accompanied the high frequency firing [ $33.0 \pm 4.9$  Hz in the first second (1 s)]. This burst of APs was correlated with the appearance of the first  $[\text{Ca}^{2+}]_i$  peak (Fig. 1). Further depolarization caused a rapid decrease in AP frequency to



9.0 ± 2.4 Hz at an  $E_m$  of  $-39.9 \pm 4.1$  mV (P1, 10th s, average time of the first  $[Ca^{2+}]_i$  peak). Plateau potential reached  $-36.6 \pm 3.7$  mV (firing rate:  $1.6 \pm 0.7$  Hz) at 80th s of the veratridine response (P2; average time of the second  $[Ca^{2+}]_i$  peak). The depolarization plateau finished abruptly, but its length varied considerably between experiments ( $382.5 \pm 103.6$  s).

#### Veratridine evokes a persistent Na<sup>+</sup> influx

Intracellular Na<sup>+</sup> dynamics following veratridine application (10 μM, 1 min) were measured by SBFI/AM, a dye sensitive to Na<sup>+</sup>. Electric field stimulation (fs) evoked a TTX- and stimulus strength-dependent Na<sup>+</sup> spike in CA1 pyramidal cells (Fig. 2a and c). Compared with the spike-type fs-evoked response, veratridine treatment induced a long-lasting, massive  $[Na^+]_i$  increase (Fig. 2c and d). This persistent Na<sup>+</sup> influx (peak:  $39.7 \pm 8.6$  mM,  $n = 14/6/4$ ) was monophasic and slowly returned to baseline. The resting  $[Na^+]_i$  was  $7.3 \pm 1.3$  mM. Calculation of  $[Na^+]_i$  was based on *in situ* calibration performed after every individual experiment (see Materials and methods).

#### VGCCs, plasma membrane NCX, and mitochondria are the sources of the veratridine-evoked $[Ca^{2+}]_i$ elevation

To explore the mechanism of  $[Ca^{2+}]_i$  elevation, we first examined the role of VGCCs. Inhibition of VGSC inactivation by veratridine induced firing of pyramidal neurons (Fig. 1b) making VGCCs a plausible candidate. CdCl<sub>2</sub>, which non-selectively and efficiently inhibits all types of VGCCs at 100 μM, abolished the first peak of the veratridine-evoked  $[Ca^{2+}]_i$  response (peak<sub>1</sub> =  $28.8 \pm 6.6$  nM vs. veratridine alone;  $p < 0.001$ ;  $n = 26/9/4$ ; Figs 3b and 4a). The effect of CdCl<sub>2</sub> on the second peak cannot be measured in our experimental model, because Cd<sup>2+</sup> enters the cells through the opened VGCCs and intracellular Cd<sup>2+</sup> increases fura-2 fluorescence ratio (Hinkle *et al.* 1992). To confirm the

**Fig. 3** Sources of intracellular Ca<sup>2+</sup> elevation resulting from the inhibition of VGSC inactivation by veratridine. Representative traces show the effect of inhibition of (a) NMDA and AMPA/Kainate receptors (AP-5, 50 μM and CNQX 30 μM, respectively), (b) VGCCs by the non-specific blocker CdCl<sub>2</sub> (100 μM) or cocktail of selective inhibitors (10 μM nifedipine, 100 μM NiCl<sub>2</sub> and 100 nM ω-conotoxin-MVIIIC), (c) plasma membrane NCX (10 μM KB-R7943), (d) mitochondrial function by CCCP (1 μM) and mitochondrial Ca<sup>2+</sup> release by mNCX inhibitor CGP-37157 (10 μM) and mPTP inhibitor CsA (1 μM), (e) mitochondrial function without rapid ATP depletion (1 μM CCCP and 10 μM oligomycin), and (f) ER Ca<sup>2+</sup>-ATPase (1 μM thapsigargin). Drug perfusion began 15 min before veratridine administration and was maintained throughout the experiment, except perfusion of the VGCC inhibitory cocktail, which was started at least 20 min before veratridine. Arrows indicate the beginning of veratridine (10 μM) action (control; thin gray line). Traces recorded in the presence of inhibitors are shown with thick black or gray lines.

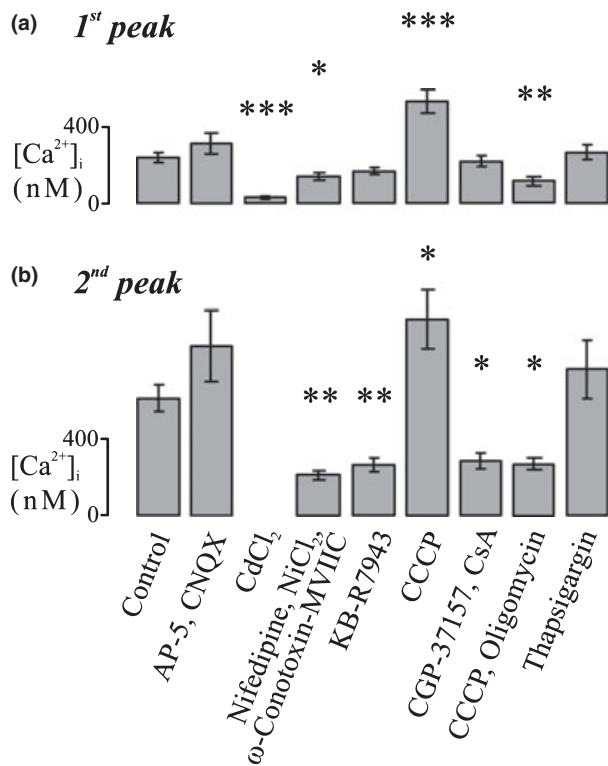


**Fig. 4** Statistical analysis of the  $\text{Ca}^{2+}$  elevation induced by veratridine. VGCCs, NCX, and mitochondria all contributed to the persistent  $\text{Na}^+$  influx-evoked  $[\text{Ca}^{2+}]_i$  elevation following veratridine (10  $\mu\text{M}$ , 1 min) application, whereas the ER did not play a significant role in the process. Bar graphs show the averages  $\pm$  SEM with significant differences during both the first (a) and the second (b) peaks. Legends, indicating treatments, apply to both a and b. Intracellular  $\text{CdCl}_2$  interacts with *fura-2* and was therefore excluded from diagram B (see Materials and methods). \* $p < 0.05$ ; \*\* $p < 0.01$ ; \*\*\* $p < 0.001$ .

effect of VGCC inhibition on the first peak and to circumvent the above-mentioned technical limitation in exploring VGCCs' role in the second peak, we next used a cocktail of VGCC inhibitors that do not interfere with *fura-2* fluorescence. The cocktail contained nifedipine (10  $\mu\text{M}$ ) the L-type,  $\text{NiCl}_2$  (100  $\mu\text{M}$ ) the R- and T-type and  $\omega$ -conotoxin-MVIIIC ( $\omega$ -CTx-MVIIIC; 100 nM) the N- and P/Q-type VGCC inhibitor (Hillyard *et al.* 1992; Randall and Tsien 1995; Catterall *et al.* 2005) because all of these VGCCs are present on the somata of CA1 pyramidal neurons (Magee and Johnston 1995). Preperfusion of this cocktail at least 20 min before veratridine administration significantly reduced both peaks (peak<sub>1</sub> = 141.6  $\pm$  18.5 nM vs. veratridine alone;  $p < 0.05$ ; peak<sub>2</sub> = 212.2  $\pm$  25.3 nM vs. veratridine alone;  $p < 0.01$ ;  $n = 21/8/7$ ; Figs 3b, 4a and b). This inhibitory cocktail blocked the electric field stimulation-evoked  $\text{Ca}^{2+}$  response (41.1  $\pm$  0.06% inhibition,  $p < 0.01$ , Tukey *post-hoc* test,  $n = 24/8/6$ ), although not as efficiently as  $\text{CdCl}_2$  (93.4  $\pm$  0.03% inhibition,  $p < 0.001$ , Tukey *post-hoc* test,

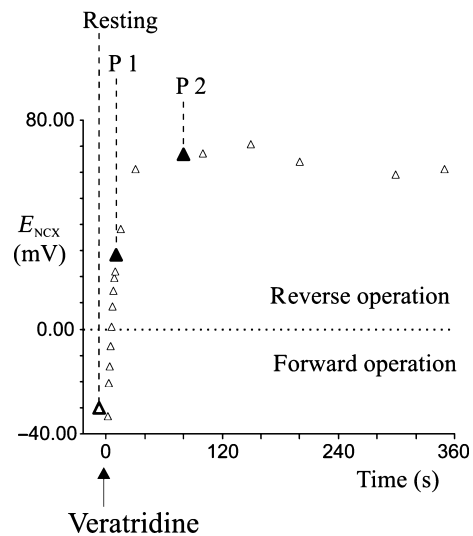


**Fig. 5** Electrochemical driving force for  $\text{Ca}^{2+}$  movement through NCX ( $E_{\text{NCX}}$ ) as a function of time after veratridine application. Actual points of the trace were calculated by using the equation  $E_{\text{NCX}} = E_m - 3E_{\text{Na}^+} + 2E_{\text{Ca}^{2+}}$ , where  $E_m$  is the membrane potential,  $E_{\text{Na}^+}$  and  $E_{\text{Ca}^{2+}}$  are the equilibrium potentials of  $\text{Na}^+$  and  $\text{Ca}^{2+}$ , respectively, both calculated by the Nernst equation. Values for  $[\text{Na}^+]_i$  and  $[\text{Ca}^{2+}]_i$  used in the Nernst equation were averages from the appropriate experiments at the appropriate time points, similarly to  $E_m$  values. Extracellular  $[\text{Na}^+]$  and  $[\text{Ca}^{2+}]$  were the concentrations of these ions in the perfusion buffer. The arrow indicates the start of the veratridine response. The large blank triangle shows resting  $E_{\text{NCX}}$ . Large black triangles (P1, P2) are the values of  $E_{\text{NCX}}$  at the average time points of the first and the second  $[\text{Ca}^{2+}]_i$  peak (10th and 80th s of veratridine response, respectively). Small blank triangles give  $E_{\text{NCX}}$  dynamics at higher temporal resolution. The dashed line at zero level of  $E_{\text{NCX}}$  shows the turning point of plasma membrane NCX. Positive values indicate reverse operation; negative values indicate forward operation.

$n = 15/5/4$ ). In spite of the lower efficiency, use of this inhibitory cocktail is appropriate when exploring the involvement of VGCCs in the  $\text{Ca}^{2+}$  response.

The increase in  $[\text{Na}^+]_i$  in our experiments (32.5  $\pm$  8.57 mM) during veratridine application (Fig. 2d) raised the possibility of  $[\text{Ca}^{2+}]_i$  elevation resulting from the reversal of plasma membrane NCX. We therefore tested the effect of KB-R7943 (10  $\mu\text{M}$ ), an inhibitor of the plasma membrane NCX (predominantly of the reverse operation; Iwamoto *et al.* 1996). All three types of NCX (NCX1-3) are found in hippocampal CA1 pyramidal neurons and are sensitive to 10  $\mu\text{M}$  KB-R7943 (Iwamoto and Shigekawa 1998; Minelli *et al.* 2007). Application of KB-R7943 did not affect the first peak (peak<sub>1</sub> = 169.8  $\pm$  17.2 nM vs. veratridine alone;  $p > 0.05$ ;  $n = 28/8/6$ ) but significantly reduced the second peak (peak<sub>2</sub> = 265.0  $\pm$  38.4 nM vs. veratridine alone;  $p < 0.01$ ;  $n = 28/8/6$ ; Figs 3c, 4a and b), showing the role of NCX in the second peak of  $[\text{Ca}^{2+}]_i$  elevation. Furthermore, we calculated the electrochemical driving force

for Ca<sup>2+</sup> movement through NCX ( $E_{\text{NCX}}$ ) with high temporal resolution to see the dynamics of NCX activity (Fig. 5). We used the following equation:  $E_{\text{NCX}} = E_m - 3E_{\text{Na}^+} + 2E_{\text{Ca}^{2+}}$ , where  $E_m$  is the membrane potential (see Fig. 1b),  $E_{\text{Na}^+}$  and  $E_{\text{Ca}^{2+}}$  are the equilibrium potentials for Na<sup>+</sup> and Ca<sup>2+</sup>, respectively, calculated from the extracellular and intracellular ion concentrations using the Nernst equation. We assumed constant extracellular concentrations of Na<sup>+</sup> (153.25 mM) and Ca<sup>2+</sup> (2 mM) based on the composition of the perfusion buffer.  $[\text{Na}^+]_i$  and  $[\text{Ca}^{2+}]_i$  are averages of veratridine responses at certain characteristic time points. Resting  $E_{\text{NCX}}$  was  $-30.22$  mV ( $E_m = -64.00 \pm 1.46$  mV;  $[\text{Na}^+]_i = 7.25 \pm 1.30$  mM;  $[\text{Ca}^{2+}]_i = 56.79 \pm 3.88$  nM) and remained in the negative range until 5 s after the start of veratridine response, indicating a forward operation. At 5 s,  $E_{\text{NCX}}$  exceeded zero and reached  $0.99$  mV ( $E_m = -44.75 \pm 3.15$  mV;  $[\text{Na}^+]_i = 13.46 \pm 1.95$  mM;  $[\text{Ca}^{2+}]_i = 228.02 \pm 23.25$  nM). After 5 s of veratridine response, i.e., during both the first ( $E_m = -39.87 \pm 4.11$  mV;  $[\text{Na}^+]_i = 18.43 \pm 3.18$  mM;  $[\text{Ca}^{2+}]_i = 241.5 \pm 24.87$  nM) and the second ( $E_m = -36.64 \pm 3.69$  mV;  $[\text{Na}^+]_i = 39.72 \pm 8.57$  mM;  $[\text{Ca}^{2+}]_i = 616.24 \pm 68.88$  nM)  $[\text{Ca}^{2+}]_i$  peaks,  $E_{\text{NCX}}$  permanently resided in the positive range (28.59 and 66.91 mV, respectively; i.e., NCX were operating in the reverse mode). Our result shows that a 5 s of pyramidal neuron firing, caused by inhibition of VGSC inactivation results in a change in the electrochemical potential that reverses NCX operation. This result is consistent with Bouron and Reuter's theoretical calculation (Bouron and Reuter 1996). Operation of NCX in both forward and reverse mode during the first  $[\text{Ca}^{2+}]_i$  peak may explain why KB-R7943 had no significant effect on this peak. Conversely, KB-R7943 significantly inhibited the second peak, when NCX was operating exclusively in the reverse mode and had a higher driving force.

Mitochondria are also primary players in shaping intracellular Ca<sup>2+</sup> responses of cells evoked by either physiological or pathological stimuli (Babcock and Hille 1998). To test their role in veratridine-evoked  $[\text{Ca}^{2+}]_i$  elevation, first we inhibited mitochondrial function by the application of CCCP (1  $\mu\text{M}$ ). As a protonophore, CCCP dissipates mitochondrial membrane potentials and decreases the electrochemical gradient, thus preventing Ca<sup>2+</sup> influx (Ca<sup>2+</sup> sequestration) into the mitochondrial matrix. When applied prior to veratridine, it altered the biphasic characteristic of the  $[\text{Ca}^{2+}]_i$  elevation to a monophasic plateau and caused a significant increase of  $[\text{Ca}^{2+}]_i$  during both phases (peak<sub>1</sub> =  $544.8 \pm 61.0$  nM vs. veratridine alone;  $p < 0.001$ ; peak<sub>2</sub> =  $1039.0 \pm 154.06$  nM vs. veratridine alone;  $p < 0.05$ ;  $n = 11/5/5$ ; Figs 3d, 4a and b). To further investigate the role of mitochondria in veratridine-evoked  $[\text{Ca}^{2+}]_i$  elevation, we inhibited mitochondrial Ca<sup>2+</sup> release via the combined administration of CGP-37157 (10  $\mu\text{M}$ ) and CsA (1  $\mu\text{M}$ ), specific inhibitors of mitochondrial NCX (Cox *et al.* 1993) and the mitochondrial permeability transition pore (mPTP

(Crompton *et al.* 1988) at these concentrations, respectively. These inhibitors did not influence the first peak (peak<sub>1</sub> =  $220.9 \pm 27.3$  nM vs. veratridine alone;  $p > 0.05$ ;  $n = 25/11/6$ ) but significantly inhibited the second (peak<sub>2</sub> =  $286.6 \pm 43.1$  nM vs. veratridine alone;  $p < 0.05$ ;  $n = 25/11/6$ ; see Figs 3d, 4a and b). In order to exclude the possible aspecific effect of CGP-37157 on plasmalemmal NCX (Czyz and Kiedrowski 2003) we repeated the mitochondrial Ca<sup>2+</sup> release inhibiting experiments in the presence of KB-R7943. The additional drop in the veratridine-induced  $[\text{Ca}^{2+}]_i$  elevation (peak<sub>2</sub> =  $97.6 \pm 17.6$  nM vs. KB-R7943 or CGP-37157 + CsA;  $p < 0.05$ ; Scheffe *post-hoc* test;  $n = 13/6/5$ ) supports that mitochondrial Ca<sup>2+</sup> release contributes to the Ca<sup>2+</sup> response. Our results suggest that during the first peak, Ca<sup>2+</sup> sequestration is the dominant action, but mitochondrial Ca<sup>2+</sup> release subsequently becomes relevant (second peak). Effect of CCCP during the second peak indicates that mitochondrial sequestration still exceeds mitochondrial Ca<sup>2+</sup> release in our hands.

Although the experiments with CCCP provide unambiguous evidence for the involvement of mitochondria in veratridine-evoked  $[\text{Ca}^{2+}]_i$  elevation, CCCP treatment also leads to rapid ATP depletion due to reversal of  $F_1F_0$  ATP synthase (Budd and Nicholls 1996). To assess the impact of ATP depletion, we tested the effect of veratridine-evoked  $[\text{Ca}^{2+}]_i$  elevation in the presence of combined application of CCCP (1  $\mu\text{M}$ ) and oligomycin (10  $\mu\text{M}$ ), the  $F_1F_0$  ATP synthase inhibitor. Oligomycin limits ATP degradation by inhibiting the reverse operation (ATP hydrolase activity) of  $F_1F_0$  ATP synthase. CCCP + oligomycin treatment reduced significantly both  $[\text{Ca}^{2+}]_i$  peaks (peak<sub>1</sub> =  $116.5 \pm 23.1$  nM vs. veratridine alone;  $p < 0.01$ ; peak<sub>2</sub> =  $273.7 \pm 32.8$  nM vs. veratridine alone;  $p < 0.05$ ;  $n = 19/7/4$ ; Figs 3e, 4a and b). This result indicates indirectly that not only CCCP, but veratridine in itself induces ATP depletion, which, consequently, leads to inhibition of ATP-dependent processes (including extrusion of intracellular Na<sup>+</sup> and Ca<sup>2+</sup>).

The ER, another important regulator of  $[\text{Ca}^{2+}]_i$ , may also influence the veratridine-evoked  $[\text{Ca}^{2+}]_i$  elevation through Ca<sup>2+</sup>-induced Ca<sup>2+</sup> release (CICR). A major determinant of CICR contribution to the elevation of  $[\text{Ca}^{2+}]_i$  is the filling state of ER Ca<sup>2+</sup> stores (Verkhatsky 2002). Empty ER Ca<sup>2+</sup> stores prevent CICR. A simple way to empty ER Ca<sup>2+</sup> stores has already been shown in hippocampal CA1 pyramidal cells and involves the inhibition of ER Ca<sup>2+</sup>-ATPase (Garaschuk *et al.* 1997; Camello *et al.* 2002). In our experiments, the use of 1  $\mu\text{M}$  thapsigargin, the irreversible and specific blocker of ER Ca<sup>2+</sup>-ATPase (Thastrup *et al.* 1990), did not affect the peaks of veratridine-evoked  $[\text{Ca}^{2+}]_i$  elevation (peak<sub>1</sub> =  $268.4 \pm 38.2$  nM;  $p > 0.05$ ; peak<sub>2</sub> =  $768.5 \pm 153.7$  nM, both vs. veratridine alone;  $p > 0.05$ ;  $n = 18/5/3$ ; Figs 3f, 4a and b), suggesting the lack of contribution of ER Ca<sup>2+</sup> stores.

## Discussion

In the present study, we investigated (i) how the non-inactivating persistent  $\text{Na}^+$  influx influences  $[\text{Ca}^{2+}]_i$ , and (ii) the sources of this  $[\text{Ca}^{2+}]_i$  increase in the somata of hippocampal CA1 pyramidal neurons in acute rat hippocampal slices. We analyzed the membrane potential, the  $[\text{Na}^+]_i$  and the  $[\text{Ca}^{2+}]_i$  under the same experimental conditions. We evoked persistent  $\text{Na}^+$  influx by veratridine, which inhibits VGSC inactivation (Denac *et al.* 2000; Ulbricht 2005). Veratridine activates the TTX-sensitive  $I_{\text{Na,P}}$  (Ulbricht 1965, 2005; Alkadhi and Tian 1996), which may play an initiating role in certain forms of epilepsy (both in VGSC mutants and genetically normal animals; Stafstrom 2007). Veratridine has also been used as a cellular model for epileptiform activity in acute brain slices (Otoom *et al.* 1998; Otoom and Alkadhi 2000). The TTX-sensitive  $I_{\text{Na,P}}$  may have relevance in the ischemic/hypoxic cascade, as well (Lysko *et al.* 1994; Hammarstrom and Gage 1998, 2002; Banasiak *et al.* 2004).

The biphasic  $[\text{Ca}^{2+}]_i$  elevation, evoked by veratridine-induced persistent  $\text{Na}^+$  influx was extracellular  $[\text{Ca}^{2+}]_o$ - and VGSC-dependent, as we (Zelles *et al.* 2001) and others (Mulkey and Zucker 1992; Lysko *et al.* 1994) have previously shown. Veratridine exerted its excitatory action directly on the examined neurons, as its effect was not influenced by the inhibition of ionotropic glutamate receptors. This result is also emphasized by other studies (Tian *et al.* 1995; Otoom *et al.* 1998). Firing and depolarization of the imaged cell, most likely overrides the influence of connected neurons also activated by veratridine (i.e., the indirect effect). Furthermore, the veratridine-induced massive depolarization may block the exocytotic release of transmitters from presynaptic terminals (Tian *et al.* 1995; Otoom *et al.* 1998) or may attenuate dendritic information transfer to the soma (Zelles *et al.* 2006).

The result of our current-clamp measurements are consistent with previous studies that applied veratridine to brain slices, i.e., AP firing and a plateau-like depolarization (Tian *et al.* 1995; Otoom *et al.* 1998). The electrophysiological response corresponded well with the  $[\text{Ca}^{2+}]_i$  response. Voltage dependence of activation and inactivation of VGCCs suggests the accessibility of all types of VGCCs during the first and R-, N-, P/Q- and L-type VGCCs during the second peak for activation in the somata of CA1 pyramidal neurons (Magee and Johnston 1995). All types of VGCCs are present (L- and N-type in the highest density) on the somata of CA1 pyramidal neurons (Magee and Johnston 1995). Both  $[\text{Ca}^{2+}]_i$  peaks were VGCC-dependent as shown by  $\text{Cd}^{2+}$  and the cocktail of inhibitors blocking all types of VGCCs. Because  $\text{Cd}^{2+}$  hampers  $[\text{Ca}^{2+}]_i$  measurement in its later phase (see Results and Hinkle *et al.* 1992) we only evaluated its inhibitory action during the first peak.

The inhibitory effect of  $\text{Cd}^{2+}$  during the first peak was stronger than that of the cocktail. This affect was likely

because of the incomplete block of N- and P/Q-type VGCCs by the applied concentration of  $\omega$ -CTx-MV1C (Hillyard *et al.* 1992; Sather *et al.* 1993; Randall and Tsien 1995). Since the occlusion of VGCCs was not our aim, the use of higher concentrations of  $\omega$ -CTx was not necessary. Contribution of VGCCs to the free cytosolic  $[\text{Ca}^{2+}]_i$  during the second peak may also have an indirect component. The  $\text{Ca}^{2+}$  that entered the cell through VGCCs during the first peak may have been taken up by the mitochondria and could be released during the second peak.

According to Iwamoto and Shigekawa (1998) a specific effect of  $\text{Ni}^{2+}$  on plasmalemmal NCX emerges at very low extracellular  $[\text{Ca}^{2+}]_o$  ( $[\text{Ca}^{2+}]_o$ ). It is well-recognized that there is a large decrease in  $[\text{Ca}^{2+}]_o$  attributable to influx of  $\text{Ca}^{2+}$  during epileptic seizures, ischemia, spreading depression or following activation of  $\text{Ca}^{2+}$ -permeable ion channels (e.g., Hansen and Zeuthen 1981; Heinemann *et al.* 1986; Pumain *et al.* 1987; Arens *et al.* 1992). The magnitude of  $\text{Ca}^{2+}$  drop depends on the type, strength and duration of the stimulus or even on the area or layer of the brain. In studies similar to our one, i.e., when veratridine (10–30  $\mu\text{M}$ ) was applied to hippocampal slices and the  $\text{Ca}^{2+}$ -sensitive microelectrode was positioned in the CA1 pyramidal layer (Ashton *et al.* 1990, 1997), much longer application of the alkaloid (20–25 min vs. our 1 min perfusion) was needed to evoke a spreading depression which can produce for a short time the magnitude of  $[\text{Ca}^{2+}]_o$  decrease necessary for inhibition of NCX by 100  $\mu\text{M}$   $\text{Ni}^{2+}$ . However, the possible implication of plasma membrane NCX inhibition by  $\text{Ni}^{2+}$  in the effect of the VGCC inhibitory cocktail during the second peak cannot be excluded.

The increase of  $[\text{Na}^+]_i$ , as a result of veratridine administration, has already been shown before in synaptosomal preparations (Deri and Adam-Vizi 1993) and tissue cultures (Rose and Ransom 1997), but not in brain slices. The magnitude of  $[\text{Na}^+]_i$  increase that we measured in our experiments was more than 30 mM, and thus should be sufficient for reversing the operation of the NCX. According to the calculation of Bouron and Reuter, based on data taken from the literature and not on their own measurements, a 5 mM increase in  $[\text{Na}^+]_i$  is sufficient for the reversal (Bouron and Reuter 1996). Our own calculation of the driving force, based on the direct measurement of  $[\text{Na}^+]_i$ ,  $[\text{Ca}^{2+}]_i$  and  $E_m$ , confirmed this assumption. Expression of  $E_{\text{NCX}}$  as a function of time also revealed that the transport of  $\text{Ca}^{2+}$  into the cell, caused by the reversal of NCX, appeared after a forward mode of operation (transporting  $\text{Ca}^{2+}$  out) in the first 5 s of the veratridine response. The lack of effect of the NCX inhibitor KB-R7943 on the first peak suggests that the transport of  $\text{Ca}^{2+}$  both into and out of the cells and the relatively weaker driving force during this phase resulted in an insignificant net effect on  $[\text{Ca}^{2+}]_i$ . Conversely, both  $E_{\text{NCX}}$  data and the inhibition by KB-R7943 suggested that the reversal of NCX played a

substantial role in the later phases of persistent Na<sup>+</sup> influx-evoked [Ca<sup>2+</sup>]<sub>i</sub> elevation (second [Ca<sup>2+</sup>]<sub>i</sub> peak; Mulkey and Zucker 1992; Saleh *et al.* 2005).

KB-R7943 has been shown to have some non-specific effects. Since the VGCC-dependent first peak of [Ca<sup>2+</sup>]<sub>i</sub> was not affected by KB-R7943, the non-specific L-type VGCC inhibitory action of KB-R7943 (Matsuda *et al.* 2001; Dietz *et al.* 2007) seems to be not significant in our experimental conditions. As mentioned, all types of VGCCs are present on the somata of CA1 pyramidal neurons (Magee and Johnston 1995). Inhibition of NMDA-receptors (Sobolevsky and Khodorov 1999) or CICR (Arakawa *et al.* 2000) by KB-R7943 were not involved in our experiments, because neither the NMDA-receptor inhibitor AP-5 nor the Ca<sup>2+</sup>-ATPase inhibitor thapsigargin had any effect on the [Ca<sup>2+</sup>]<sub>i</sub> response. However, inhibition of Ca<sup>2+</sup> influx through the TRPC channels by KB-R7943 cannot be excluded (Kraft 2007). Of the TRPC channels that are inhibited by KB-R7943, TRPC3 and TRPC5 channels are prominently expressed in CA1 neurons.

We have also considered the possible contribution of intracellular Ca<sup>2+</sup> pools. In order to test [Ca<sup>2+</sup>]<sub>i</sub> buffering role of mitochondria (Werth and Thayer 1994; Babcock and Hille 1998; Berridge *et al.* 2000) in the veratridine-evoked Ca<sup>2+</sup> response, we first inhibited both the Ca<sup>2+</sup> uptake and release of mitochondria by the protonophore CCCP. Effect of CCCP on the second peak suggests that, in spite of the increasing amount of mitochondrial Ca<sup>2+</sup> release, mitochondrial Ca<sup>2+</sup> sequestration still exceeds mitochondrial Ca<sup>2+</sup> release. Second, to see the relevance of mitochondrial Ca<sup>2+</sup> release separately, we inhibited its two components. The mNCX of excitable cells is the prevailing Ca<sup>2+</sup> extrusion route (Blaustein and Lederer 1999). The extent of [Na<sup>+</sup>]<sub>i</sub> elevation, generated by the persistent Na<sup>+</sup> influx in our experiments, induces its operation (Rizzuto *et al.* 2000). The other route of mitochondrial Ca<sup>2+</sup> release is the mPTP, which is a central participant in several pathological and possibly physiological processes (Babcock and Hille 1998; Rizzuto *et al.* 2000). The first peak was unaffected by CGP-37157 plus CsA, which suggests the exclusive role of sequestration during the first Ca<sup>2+</sup> peak, contrary to the second that involved both Ca<sup>2+</sup> sequestration and release. The finding that Ca<sup>2+</sup>-free media abolished elevation of [Ca<sup>2+</sup>]<sub>i</sub> suggests the extracellular origin of mitochondrial Ca<sup>2+</sup> release (Mulkey and Zucker 1992).

Although the effect of CGP-37157 on certain isoforms of plasma membrane NCX was suggested, its effect was considered not significant at 10 μM (Cox *et al.* 1993; Czyz and Kiedrowski 2003). The compound is widely used as a specific mNCX inhibitor even in 15 μM in brain slices (Kovacs *et al.* 2005) or in 10 μM in neuronal cultures (Medvedeva *et al.* 2008; Ryan *et al.* 2009). These data are also supported by our own experiments showing that inhibition of plasmalemmal NCX by CGP-37157 (Cox *et al.*

1993) does not play a significant role in the inhibition of veratridine-induced [Ca<sup>2+</sup>]<sub>i</sub> elevation by the drug because simultaneous inhibition of plasmalemmal NCX by KB-R7943 causes an additional drop in [Ca<sup>2+</sup>]<sub>i</sub>.

The CCCP + oligomycin experiments support that veratridine by itself can deplete ATP. Scott and Nicholls have shown that the enhanced Na<sup>+</sup> and K<sup>+</sup> cycling and consequent ATP utilization should be the reason for this (Scott and Nicholls 1980). Salvage of ATP by oligomycin, inhibiting F<sub>1</sub>F<sub>0</sub> ATP synthase reversal especially in mitochondria near the plasma membrane, which are more heavily affected by Ca<sup>2+</sup> influx and mitochondrial depolarization (Pivovarov *et al.* 1999), may contribute to the normal Na<sup>+</sup>-K<sup>+</sup> ATPase and plasma membrane Ca<sup>2+</sup> pump activity. Sustained activity of the Na<sup>+</sup>-K<sup>+</sup> ATPase and plasma membrane Ca<sup>2+</sup> pump may be responsible for the reduced Ca<sup>2+</sup> response following veratridine application in the presence of oligomycin.

We also investigated the contribution of CICR with thapsigargin, which did not influence the peaks of the [Ca<sup>2+</sup>]<sub>i</sub> response. The reason for this may be that resting ER Ca<sup>2+</sup> stores contain only a small amount of releasable Ca<sup>2+</sup> compared to global somatic Ca<sup>2+</sup> transients and CICR occurs locally in small Ca<sup>2+</sup> microdomains (Kiedrowski and Costa 1995; Berridge 1998; Sandler and Barbara 1999). Thus, CICR may significantly influence the Ca<sup>2+</sup> transients evoked by one or a few APs (Sandler and Barbara 1999) but not large (global) Ca<sup>2+</sup> loads of the cytosol (e.g., after the reversal of the high capacity NCX) in response to epileptiform activity or ischemia.

Evidence accumulated in the recent years clearly indicates that changes in [Ca<sup>2+</sup>]<sub>i</sub> and Ca<sup>2+</sup> homeostatic mechanisms are playing a prominent role in the genesis and maintenance of acquired epilepsy (DeLorenzo *et al.* 2006). Activation of the persistent Na<sup>+</sup> current is also known as a cellular mechanism underlying certain epileptic phenotypes (Denac *et al.* 2000; Meisler and Kearney 2005; Stafstrom 2007). Its induction in brain slices by veratridine is used as an epileptic model (Tian *et al.* 1995; Otoom *et al.* 1998). Thorough understanding of the connections between the two mechanisms is required for the understanding of the development of acquired epilepsy and for inventing novel therapeutic tools to prevent or even cure this disease.

Our results suggest the following linkage of events after activation of the persistent Na<sup>+</sup> current. Extracellular Ca<sup>2+</sup> enters the cytosol through VGCCs (first and second peak) and the plasma membrane NCX (second peak). Both Ca<sup>2+</sup> peaks are in the submicromolar range, where mitochondrial Ca<sup>2+</sup> uptake comes into play (Babcock and Hille 1998; Colegrove *et al.* 2000). After Ca<sup>2+</sup> sequestration (during both the first and second peak), mitochondrial Ca<sup>2+</sup> is released back to the cytosol slowly (second peak; Berridge *et al.* 2000). A better understanding of the effect of persistent, non-inactivating Na<sup>+</sup> influx on the dysregulation of cellular Ca<sup>2+</sup>

homeostasis has physiological, pathophysiological and pharmacological relevance.

## Acknowledgments

This work was supported by the Hungarian Medical Research Foundation (576/2006) and the Hungarian Research Found (OTKA TS 049868; OTKA NK 72959). Authors thank Albert Barth and Szilárd Szabó for their technical advices and Kerry Delaney for helpful discussion and useful suggestion concerning data presentation.

## References

- Alkadhi K. A. and Tian L. M. (1996) Veratridine-enhanced persistent sodium current induces bursting in CA1 pyramidal neurons. *Neuroscience* **71**, 625–632.
- Alzheimer C., Schwandt P. C. and Crill W. E. (1993) Modal gating of  $\text{Na}^+$  channels as a mechanism of persistent  $\text{Na}^+$  current in pyramidal neurons from rat and cat sensorimotor cortex. *J. Neurosci.* **13**, 660–673.
- Arakawa N., Sakaue M., Yokoyama I., Hashimoto H., Koyama Y., Baba A. and Matsuda T. (2000) KB-R7943 inhibits store-operated  $\text{Ca}^{2+}$  entry in cultured neurons and astrocytes. *Biochem. Biophys. Res. Commun.* **279**, 354–357.
- Arens J., Stabel J. and Heinemann U. (1992) Pharmacological properties of excitatory amino acid induced changes in extracellular calcium concentration in rat hippocampal slices. *Can. J. Physiol. Pharmacol.* **70**(Suppl.), S194–205.
- Ashton D., Willems R., Marrannes R. and Janssen P. A. (1990) Extracellular ions during veratridine-induced neurotoxicity in hippocampal slices: neuroprotective effects of flunarizine and tetrodotoxin. *Brain Res.* **528**, 212–222.
- Ashton D., Willems R., Wynants J., Van Reempts J., Marrannes R. and Clincke G. (1997) Altered  $\text{Na}^{+}$ -channel function as an in vitro model of the ischemic penumbra: action of lubeluzole and other neuroprotective drugs. *Brain Res.* **745**, 210–221.
- Babcock D. F. and Hille B. (1998) Mitochondrial oversight of cellular  $\text{Ca}^{2+}$  signaling. *Curr. Opin. Neurobiol.* **8**, 398–404.
- Banasiak K. J., Burenkova O. and Haddad G. G. (2004) Activation of voltage-sensitive sodium channels during oxygen deprivation leads to apoptotic neuronal death. *Neuroscience* **126**, 31–44.
- Bean B. P. (2007) The action potential in mammalian central neurons. *Nat. Rev. Neurosci.* **8**, 451–465.
- Berridge M. J. (1998) Neuronal calcium signaling. *Neuron* **21**, 13–26.
- Berridge M. J., Lipp P. and Bootman M. D. (2000) The versatility and universality of calcium signalling. *Nat. Rev. Neurosci.* **1**, 11–21.
- Blaustein M. P. and Lederer W. J. (1999) Sodium/calcium exchange: its physiological implications. *Physiol. Rev.* **79**, 763–854.
- Borzak S., Reers M., Arruda J., Sharma V. K., Sheu S. S., Smith T. W. and Marsh J. D. (1992)  $\text{Na}^+$  efflux mechanisms in ventricular myocytes: measurement of  $[\text{Na}^+]_i$  with  $\text{Na}^{+}$ -binding benzofuran isophthalate. *Am. J. Physiol.* **263**, H866–874.
- Bouron A. and Reuter H. (1996) A role of intracellular  $\text{Na}^+$  in the regulation of synaptic transmission and turnover of the vesicular pool in cultured hippocampal cells. *Neuron* **17**, 969–978.
- Budd S. L. and Nicholls D. G. (1996) A reevaluation of the role of mitochondria in neuronal  $\text{Ca}^{2+}$  homeostasis. *J. Neurochem.* **66**, 403–411.
- Camello C., Lomax R., Petersen O. H. and Tepikin A. V. (2002) Calcium leak from intracellular stores—the enigma of calcium signalling. *Cell Calcium* **32**, 355–361.
- Catterall W. A., Perez-Reyes E., Snutch T. P. and Striessnig J. (2005) International Union of Pharmacology. XLVIII. Nomenclature and structure-function relationships of voltage-gated calcium channels. *Pharmacol. Rev.* **57**, 411–425.
- Colegrove S. L., Albrecht M. A. and Friel D. D. (2000) Dissection of mitochondrial  $\text{Ca}^{2+}$  uptake and release fluxes in situ after depolarization-evoked  $[\text{Ca}^{2+}]_i$  elevations in sympathetic neurons. *J. Gen. Physiol.* **115**, 351–370.
- Cox D. A., Conforti L., Sperelakis N. and Matlib M. A. (1993) Selectivity of inhibition of  $\text{Na}^{+}$ - $\text{Ca}^{2+}$  exchange of heart mitochondria by benzothiazepine CGP-37157. *J. Cardiovasc. Pharmacol.* **21**, 595–599.
- Crill W. E. (1996) Persistent sodium current in mammalian central neurons. *Annu. Rev. Physiol.* **58**, 349–362.
- Crompton M., Ellinger H. and Costi A. (1988) Inhibition by cyclosporin A of a  $\text{Ca}^{2+}$ -dependent pore in heart mitochondria activated by inorganic phosphate and oxidative stress. *Biochem. J.* **255**, 357–360.
- Czys A. and Kiedrowski L. (2003) Inhibition of plasmalemmal  $\text{Na}^{+}/\text{Ca}^{2+}$  exchange by mitochondrial  $\text{Na}^{+}/\text{Ca}^{2+}$  exchange inhibitor 7-chloro-5-(2-chlorophenyl)-1,5-dihydro-4,1-benzothiazepin-2(3H)-one (CGP-37157) in cerebellar granule cells. *Biochem. Pharmacol.* **66**, 2409–2411.
- DeLorenzo R. J., Sun D. A. and Deshpande L. S. (2006) Erratum to “Cellular mechanisms underlying acquired epilepsy: the calcium hypothesis of the induction and maintenance of epilepsy.” [Pharmacol. Ther. 105(3) (2005) 229–266]. *Pharmacol. Ther.* **111**, 288–325.
- Denac H., Mevissen M. and Scholtysik G. (2000) Structure, function and pharmacology of voltage-gated sodium channels. *Naunyn Schmiedebergs Arch. Pharmacol.* **362**, 453–479.
- Deri Z. and Adam-Vizi V. (1993) Detection of intracellular free  $\text{Na}^+$  concentration of synaptosomes by a fluorescent indicator,  $\text{Na}^{+}$ -binding benzofuran isophthalate: the effect of veratridine, ouabain, and alpha-latrotoxin. *J. Neurochem.* **61**, 818–825.
- Diarra A., Sheldon C. and Church J. (2001) In situ calibration and  $[\text{H}^+]$  sensitivity of the fluorescent  $\text{Na}^+$  indicator SBFI. *Am. J. Physiol. Lung Cell. Mol. Physiol.* **280**, C1623–1633.
- Dietz R. M., Kiedrowski L. and Shuttleworth C. W. (2007) Contribution of  $\text{Na}^{+}/\text{Ca}^{2+}$  exchange to excessive  $\text{Ca}^{2+}$  loading in dendrites and somata of CA1 neurons in acute slice. *Hippocampus* **17**, 1049–1059.
- Fekete A., Vizi E. S., Kovacs K. J., Lendvai B. and Zelles T. (2008) Layer-specific differences in reactive oxygen species levels after oxygen-glucose deprivation in acute hippocampal slices. *Free Radic. Biol. Med.* **44**, 1010–1022.
- French C. R., Sah P., Buckett K. J. and Gage P. W. (1990) A voltage-dependent persistent sodium current in mammalian hippocampal neurons. *J. Gen. Physiol.* **95**, 1139–1157.
- Garaschuk O., Yaari Y. and Konnerth A. (1997) Release and sequestration of calcium by ryanodine-sensitive stores in rat hippocampal neurons. *J. Physiol.* **502**, 13–30.
- Grynkiewicz G., Poenie M. and Tsien R. Y. (1985) A new generation of  $\text{Ca}^{2+}$  indicators with greatly improved fluorescence properties. *J. Biol. Chem.* **260**, 3440–3450.
- Hammarstrom A. K. and Gage P. W. (1998) Inhibition of oxidative metabolism increases persistent sodium current in rat CA1 hippocampal neurons. *J. Physiol.* **510**, 735–741.
- Hammarstrom A. K. and Gage P. W. (2002) Hypoxia and persistent sodium current. *Eur. Biophys. J.* **31**, 323–330.
- Hansen A. J. and Zeuthen T. (1981) Extracellular ion concentrations during spreading depression and ischemia in the rat brain cortex. *Acta Physiol. Scand.* **113**, 437–445.
- Harootunian A. T., Kao J. P., Eckert B. K. and Tsien R. Y. (1989) Fluorescence ratio imaging of cytosolic free  $\text{Na}^+$  in individual fibroblasts and lymphocytes. *J. Biol. Chem.* **264**, 19458–19467.

- Heinemann U., Konnerth A., Pumain R. and Wadman W. J. (1986) Extracellular calcium and potassium concentration changes in chronic epileptic brain tissue. *Adv. Neurol.* **44**, 641–661.
- Hillyard D. R., Monje V. D., Mintz I. M. *et al.* (1992) A new Conus peptide ligand for mammalian presynaptic Ca<sup>2+</sup> channels. *Neuron* **9**, 69–77.
- Hinkle P. M., Shanshala E. D. II and Nelson E. J. (1992) Measurement of intracellular cadmium with fluorescent dyes. Further evidence for the role of calcium channels in cadmium uptake. *J. Biol. Chem.* **267**, 25553–25559.
- Iwamoto T. and Shigekawa M. (1998) Differential inhibition of Na<sup>+</sup>/Ca<sup>2+</sup> exchanger isoforms by divalent cations and isothiourea derivative. *Am. J. Physiol.* **275**, C423–430.
- Iwamoto T., Watano T. and Shigekawa M. (1996) A novel isothiourea derivative selectively inhibits the reverse mode of Na<sup>+</sup>/Ca<sup>2+</sup> exchange in cells expressing NCX1. *J. Biol. Chem.* **271**, 22391–22397.
- Kiedrowski L. and Costa E. (1995) Glutamate-induced destabilization of intracellular calcium concentration homeostasis in cultured cerebellar granule cells: role of mitochondria in calcium buffering. *Mol. Pharmacol.* **47**, 140–147.
- Kiedrowski L., Brooker G., Costa E. and Wroblewski J. T. (1994) Glutamate impairs neuronal calcium extrusion while reducing sodium gradient. *Neuron* **12**, 295–300.
- Kovacs R., Kardos J., Heinemann U. and Kann O. (2005) Mitochondrial calcium ion and membrane potential transients follow the pattern of epileptiform discharges in hippocampal slice cultures. *J. Neurosci.* **25**, 4260–4269.
- Kraft R. (2007) The Na<sup>+</sup>/Ca<sup>2+</sup> exchange inhibitor KB-R7943 potently blocks TRPC channels. *Biochem. Biophys. Res. Commun.* **361**, 230–236.
- Llinas R. and Sugimori M. (1980) Electrophysiological properties of in vitro Purkinje cell somata in mammalian cerebellar slices. *J. Physiol.* **305**, 171–195.
- Lynch J. J. III, Yu S. P., Canzoniero L. M., Sensi S. L. and Choi D. W. (1995) Sodium channel blockers reduce oxygen-glucose deprivation-induced cortical neuronal injury when combined with glutamate receptor antagonists. *J. Pharmacol. Exp. Ther.* **273**, 554–560.
- Lysko P. G., Webb C. L., Yue T. L., Gu J. L. and Feuerstein G. (1994) Neuroprotective effects of tetrodotoxin as a Na<sup>+</sup> channel modulator and glutamate release inhibitor in cultured rat cerebellar neurons and in gerbil global brain ischemia. *Stroke* **25**, 2476–2482.
- Magee J. C. and Johnston D. (1995) Characterization of single voltage-gated Na<sup>+</sup> and Ca<sup>2+</sup> channels in apical dendrites of rat CA1 pyramidal neurons. *J. Physiol.* **487**, 67–90.
- Malgouris C., Daniel M. and Doble A. (1994) Neuroprotective effects of riluzole on N-methyl-D-aspartate- or veratridine-induced neurotoxicity in rat hippocampal slices. *Neurosci. Lett.* **177**, 95–99.
- Matsuda T., Arakawa N., Takuma K. *et al.* (2001) SEA0400, a novel and selective inhibitor of the Na<sup>+</sup>-Ca<sup>2+</sup> exchanger, attenuates reperfusion injury in the in vitro and in vivo cerebral ischemic models. *J. Pharmacol. Exp. Ther.* **298**, 249–256.
- Medvedeva Y. V., Kim M. S. and Usachev Y. M. (2008) Mechanisms of prolonged presynaptic Ca<sup>2+</sup> signaling and glutamate release induced by TRPV1 activation in rat sensory neurons. *J. Neurosci.* **28**, 5295–5311.
- Meisler M. H. and Kearney J. A. (2005) Sodium channel mutations in epilepsy and other neurological disorders. *J. Clin. Invest.* **115**, 2010–2017.
- Minelli A., Castaldo P., Gobbi P., Salucci S., Magi S. and Amoroso S. (2007) Cellular and subcellular localization of Na<sup>+</sup>-Ca<sup>2+</sup> exchanger protein isoforms, NCX1, NCX2, and NCX3 in cerebral cortex and hippocampus of adult rat. *Cell Calcium* **41**, 221–234.
- Minta A. and Tsien R. Y. (1989) Fluorescent indicators for cytosolic sodium. *J. Biol. Chem.* **264**, 19449–19457.
- Mulkey R. M. and Zucker R. S. (1992) Posttetanic potentiation at the crayfish neuromuscular junction is dependent on both intracellular calcium and sodium ion accumulation. *J. Neurosci.* **12**, 4327–4336.
- Negulescu P. A. and Machen T. E. (1990) Intracellular ion activities and membrane transport in parietal cells measured with fluorescent dyes. *Methods Enzymol.* **192**, 38–81.
- Otoom S. A. and Alkadhi K. A. (2000) Action of carbamazepine on epileptiform activity of the veratridine model in CA1 neurons. *Brain Res.* **885**, 289–294.
- Otoom S., Tian L. M. and Alkadhi K. A. (1998) Veratridine-treated brain slices: a cellular model for epileptiform activity. *Brain Res.* **789**, 150–156.
- Pauwels P. J., Van Assouw H. P., Leysen J. E. and Janssen P. A. (1989) Ca<sup>2+</sup>-mediated neuronal death in rat brain neuronal cultures by veratridine: protection by flunarizine. *Mol. Pharmacol.* **36**, 525–531.
- Pivovarova N. B., Hongpaisan J., Andrews S. B. and Friel D. D. (1999) Depolarization-induced mitochondrial Ca accumulation in sympathetic neurons: spatial and temporal characteristics. *J. Neurosci.* **19**, 6372–6384.
- Pumain R., Kurcewicz I. and Louvel J. (1987) Ionic changes induced by excitatory amino acids in the rat cerebral cortex. *Can. J. Physiol. Pharmacol.* **65**, 1067–1077.
- Randall A. and Tsien R. W. (1995) Pharmacological dissection of multiple types of Ca<sup>2+</sup> channel currents in rat cerebellar granule neurons. *J. Neurosci.* **15**, 2995–3012.
- Rizzuto R., Bernardi P. and Pozzan T. (2000) Mitochondria as all-round players of the calcium game. *J. Physiol.* **529**, 37–47.
- Rose C. R. and Ransom B. R. (1997) Regulation of intracellular sodium in cultured rat hippocampal neurons. *J. Physiol.* **499**, 573–587.
- Ryan D., Drysdale A. J., Lafourcade C., Pertwee R. G. and Platt B. (2009) Cannabidiol targets mitochondria to regulate intracellular Ca<sup>2+</sup> levels. *J. Neurosci.* **29**, 2053–2063.
- Saleh S., Yeung S. Y., Prestwich S., Pucovsky V. and Greenwood I. (2005) Electrophysiological and molecular identification of voltage-gated sodium channels in murine vascular myocytes. *J. Physiol.* **568**, 155–169.
- Sandler V. M. and Barbara J. G. (1999) Calcium-induced calcium release contributes to action potential-evoked calcium transients in hippocampal CA1 pyramidal neurons. *J. Neurosci.* **19**, 4325–4336.
- Sather W. A., Tanabe T., Zhang J. F., Mori Y., Adams M. E. and Tsien R. W. (1993) Distinctive biophysical and pharmacological properties of class A (BI) calcium channel alpha 1 subunits. *Neuron* **11**, 291–303.
- Scott I. D. and Nicholls D. G. (1980) Energy transduction in intact synaptosomes. Influence of plasma-membrane depolarization on the respiration and membrane potential of internal mitochondria determined in situ. *Biochem. J.* **186**, 21–33.
- Sobolevsky A. I. and Khodorov B. I. (1999) Blockade of NMDA channels in acutely isolated rat hippocampal neurons by the Na<sup>+</sup>/Ca<sup>2+</sup> exchange inhibitor KB-R7943. *Neuropharmacology* **38**, 1235–1242.
- Stafstrom C. E. (2007) Persistent sodium current and its role in epilepsy. *Epilepsy Curr.* **7**, 15–22.
- Stafstrom C. E., Schwindt P. C. and Crill W. E. (1982) Negative slope conductance due to a persistent subthreshold sodium current in cat neocortical neurons in vitro. *Brain Res.* **236**, 221–226.
- Stafstrom C. E., Schwindt P. C., Chubb M. C. and Crill W. E. (1985) Properties of persistent sodium conductance and calcium conductance of layer V neurons from cat sensorimotor cortex in vitro. *J. Neurophysiol.* **53**, 153–170.

- Taylor C. P. (1993) Na<sup>+</sup> currents that fail to inactivate. *Trends Neurosci.* **16**, 455–460.
- Taylor C. P. and Meldrum B. S. (1995) Na<sup>+</sup> channels as targets for neuroprotective drugs. *Trends Pharmacol. Sci.* **16**, 309–316.
- Tazerart S., Vinay L. and Brocard F. (2008) The persistent sodium current generates pacemaker activities in the central pattern generator for locomotion and regulates the locomotor rhythm. *J. Neurosci.* **28**, 8577–8589.
- Thastrup O., Cullen P. J., Drobak B. K., Hanley M. R. and Dawson A. P. (1990) Thapsigargin, a tumor promoter, discharges intracellular Ca<sup>2+</sup> stores by specific inhibition of the endoplasmic reticulum Ca<sup>2+</sup>-ATPase. *Proc. Natl. Acad. Sci. USA* **87**, 2466–2470.
- Tian L. M., Ootom S. and Alkadhi K. A. (1995) Endogenous bursting due to altered sodium channel function in rat hippocampal CA1 neurons. *Brain Res.* **680**, 164–172.
- Tymianski M. and Tator C. H. (1996) Normal and abnormal calcium homeostasis in neurons: a basis for the pathophysiology of traumatic and ischemic central nervous system injury. *Neurosurgery* **38**, 1176–1195.
- Ulbricht W. (1965) Voltage Clamp Studies of Veratridinized Frog Nodes. *J. Cell Comp. Physiol.* **66**, 91–98.
- Ulbricht W. (2005) Sodium channel inactivation: molecular determinants and modulation. *Physiol. Rev.* **85**, 1271–1301.
- Verkhatsky A. (2002) The endoplasmic reticulum and neuronal calcium signalling. *Cell Calcium* **32**, 393–404.
- Werth J. L. and Thayer S. A. (1994) Mitochondria buffer physiological calcium loads in cultured rat dorsal root ganglion neurons. *J. Neurosci.* **14**, 348–356.
- White R. J. and Reynolds I. J. (1995) Mitochondria and Na<sup>+</sup>/Ca<sup>2+</sup> exchange buffer glutamate-induced calcium loads in cultured cortical neurons. *J. Neurosci.* **15**, 1318–1328.
- Willow M. and Catterall W. A. (1982) Inhibition of binding of [3H]batrachotoxinin A 20- $\alpha$ -benzoate to sodium channels by the anticonvulsant drugs diphenylhydantoin and carbamazepine. *Mol. Pharmacol.* **22**, 627–635.
- Worley P. F. and Baraban J. M. (1987) Site of anticonvulsant action on sodium channels: autoradiographic and electrophysiological studies in rat brain. *Proc. Natl. Acad. Sci. USA* **84**, 3051–3055.
- Zelles T., Franklin L., Koncz I., Lendvai B. and Zsilla G. (2001) The nootropic drug vinpocetine inhibits veratridine-induced [Ca<sup>2+</sup>]<sub>i</sub> increase in rat hippocampal CA1 pyramidal cells. *Neurochem. Res.* **26**, 1095–1100.
- Zelles T., Boyd J. D., Hardy A. B. and Delaney K. R. (2006) Branch-specific Ca<sup>2+</sup> influx from Na<sup>+</sup>-dependent dendritic spikes in olfactory granule cells. *J. Neurosci.* **26**, 30–40.